2011 50th IEEE Conference on Decision and Control and
European Control Conference (CDC-ECC)
Orlando, FL, USA, December 12-15, 2011

LTV-MPC Approach for Lateral Vehicle Guidance by Front Steering at the Limits of Vehicle Dynamics

Alexander Katriniok and Dirk Abel

Abstract— **In this paper, a linear time-varying model-based predictive controller (LTV-MPC) for lateral vehicle guidance by front steering is proposed. Due to the fact that this controller is designed in the scope of a Collision Avoidance System, it has to fulfill the requirement of an appropiate control performance at the limits of vehicle dynamics. To achieve this objective, the introduced approach employs estimations of the applied steering angle as well as the state variable trajectory to be used for successive linearization of the nonlinear prediction model over the prediction horizon. To evaluate the control performance, the proposed controller is compared to a LTV-MPC controller that uses linearizations of the nonlinear prediction model that remain unchanged over the prediction horizon. Simulation results show that an improved control performance can be achieved by the estimation based approach.**

I. INTRODUCTION

Advanced driver assistance systems (ADAS) that actively support the driver in common as well as critical driving situations are finding increasingly their way into nowadays cars. For example, Adaptive Cruise Controls (ACC) assist the driver in common driving situations in keeping a desired velocity resp. time gap to the preceding vehicle whereas antilock braking systems (ABS), electronic stability programs (ESP) or traction controls (TC) ensure that the vehicle is stabilized in critical driving situations. To look ahead, one day this will result in ADAS like Collision Avoidance Systems (CAS) that intervene autonomously to avoid an accident, see [1].

In order to enhance the performance and the field of application of actual ADAS, a reliable and precise detection of the surrounding environment is essential. For this reason, RWTH Aachen University conducts research in the field of Global Navigation Satellite System (GNSS) based ADAS. In particular, a CAS that employs a GNSS in combination with digital road maps and vehicle-to-vehicle communication is subject of ongoing research in the scope of the project "Galileo above", see [2]. The intended behavior of CAS is to keep track of surrounding vehicles and to conduct an autonomous emergency braking resp. evasion maneuver if the driver does not react appropiately and in time. The application of CAS can be separated into the tasks of sensor fusion, decision making, path planning and vehicle control. This paper will focus on the task of vehicle control and in particular on the control scheme for lateral vehicle guidance by front steering. In order to permit the driver to avoid the collision himself, a collision avoidance maneuver should be executed as late as possible. Thus, the controller must be able to stabilize the vehicle in case of high lateral accelerations and even at the limits of vehicle dynamics. For this reason, nonlinear vehicle dynamics have to be taken into account. Due to the fact that the evasion path, provided by the path planner, is known over a finite time horizon and the controller is aware of physical constraints (e.g. actuator constraints, max. feasible tire forces), a model-based predictive control strategy [3] is investigated.

In literature, several MPC-based control schemes for lateral vehicle guidance, considering the vehicle's nonlinear behavior, are proposed. For example, [4] introduces a switching model-based predictive control strategy to control the desired yaw rate which originates from the applied steering angle and current driving conditions. [5] presents a hybrid parameter-varying and a nonlinear MPC-based (NMPC) steering-only controller in the context of a side wind rejection and a double lane change scenario. [6] proposes a NMPC and a LTV-MPC approach to guide a vehicle on an a priori known path using front steering. In this paper, a LTV-MPC approach based on an extension of [6] is presented that is aimed at handling the highly nonlinear vehicle behavior at the limits of vehicle dynamics. In this regard, an estimation of the control input, i.e. the steering angle, and the state variable trajectory is determined to be used for successive linearization of the nonlinear prediction model over the prediction horizon. In order to evaluate the proposed controller, a reference LTV-MPC controller, employing linearizations that remain unchanged over the prediction horizon, is used for validation purposes. Simulation results show that an improved control performance can be achieved by the estimation based approach.

This paper is structured as follows: In section II, the applied vehicle and tire model, used for prediction purposes, is presented. Subsequently, the reference as well as the estimation based LTV-MPC controller are introduced in section III. In section IV, simulation results for a double lane change maneuver on a snow covered road are presented. Finally, section V concludes with a summary and an outlook for future works.

II. PREDICTION MODEL

In this section, the plant model to predict the vehicle's movement over the prediction horizon is presented. The nonlinear plant model that is used to validate the presented

"Galileo above" is funded by the Federal Ministry of Economics and Technology, in compliance with a resolution of the German Parliament.

A. Katriniok and D. Abel are with the Institute of Automatic Control, Department of Mechanical Engineering, RWTH Aachen University, 52074 Aachen, Germany {A.Katriniok, D.Abel}@irt.rwth-aachen.de

predictive controllers has in fact a much higher complexity and is provided by a vehicle dynamics simulation software, see section IV.

A. Vehicle model

To describe vehicle dynamics, a nonlinear single-track model according to [7] is employed. Thereby, the following assumptions are made: the height of the center of gravity (COG) is assumed to be zero, hence pitch and roll dynamics are neglected; no longitudinal forces are applied neither at the front nor at the rear tire; rolling resistances and aerodynamic drag are neglected. Furthermore, all used model parameters are explained in Table I.

$$m\dot{v}_x = m\dot{\psi}v_y - F_{y,f}\sin(\delta) \tag{1}$$

$$m\dot{v}_y = -m\dot{\psi}v_x + F_{y,f}\cos(\delta) + F_{y,r} \tag{2}$$

$$J_z\ddot{\psi} = F_{y,f}\cos(\delta)l_f - F_{y,r}l_r \tag{3}$$

$$\Delta\dot{\psi} = \dot{\psi} - \kappa\sqrt{{v_x}^2 + {v_y}^2} \tag{4}$$

$$\Delta\dot{y} = \sqrt{{v_x}^2 + {v_y}^2}\sin(\Delta\psi) + v_y \tag{5}$$

Equations (1)-(2) describe the longitudinal resp. the lateral vehicle movement with respect to the vehicle reference frame (x^V, y^V) by the Newton-Euler-Equations while (3) models the yaw dynamics. In order to predict the vehicle's movement relative to the evasion path, additional differential equations are needed, see [8]. In this regard, (4) describes the relative yaw dynamics between the vehicle's longitudinal axis and the tangent to the evasion path. Finally, the relative lateral movement between the vehicle's COG and the evasion path is modeled by (5). Obviously, the vehicle follows the evasion path in an optimal way if the lateral distance Δy is close to zero for the entire maneuver. In (1)-(3), $F_{y,f}$ resp. $F_{y,r}$ have to be replaced by the employed tire model which is introduced in the next subsection.

B. Tire model

In order to determine the lateral tire forces $F_{y,f}$ and $F_{y,r}$ in (1)-(3), an appropiate tire model is needed. Therefore, a Pacejka magic formula tire model according to [9] is employed. This semi-empirical model is used to describe

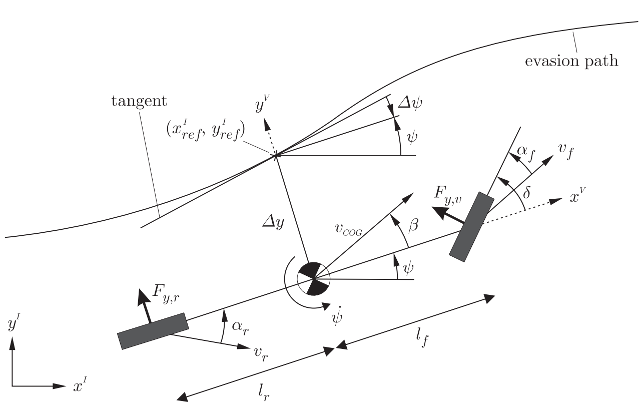

Fig. 1. Free body diagram of the employed vehicle model

TABLE I
MODEL PARAMETERS

Symbol	Description
m	Vehicle mass
J_z	Mass moment of inertia (vertical axis)
l_f, l_r	Distance between COG and front/rear axle
v_x, v_y	Longitudinal/lateral velocity at COG in veh. ref. frame
$\dot{\psi}$, ψ	Yaw rate, yaw angle
$\Delta\psi$	Difference angle between the vehicle and evasion path
Δy	Lateral distance between vehicle and evasion path
δ	Steering angle at the front axle
κ	Path's curvature at (x^I_{ref}, y^I_{ref}) (inertial ref. frame)
β	Vehicle sideslip angle
α_f, α_r	Sideslip angle at the front/rear tire
$F_{y,f}$, $F_{y,r}$	Applied lateral forces at the front/rear tire
v_{COG}	Absolute velocity at the COG
v_f, v_r	Absolute velocity at the front/rear tire

the steady-state lateral tire forces at pure cornering, i.e. no longitudinal forces are applied at the wheel. In this context, it is assumed that the vertical tire load at the front resp. the rear tire and the friction coefficient are constant. Thus, the lateral tire forces at the front resp. the rear tire in (1)-(3) can be expressed with respect to the tire sideslip angle α_f at the front resp. α_r at the rear tire as

$$F_{y,i} = D_i\sin[C_i\arctan\{B_i\alpha_i - E_i(B_i\alpha_i - \arctan(B_i\alpha_i))\}],$$
$$i \in \{f, r\} \tag{6}$$

where α_i is defined as

$$\alpha_f = \delta - \arctan((v_y + l_f\dot{\psi})/v_x), \tag{7}$$

$$\alpha_r = -\arctan((v_y - l_r\dot{\psi})/v_x) \tag{8}$$

according to [7].

C. Resulting prediction model

Finally, replacing $F_{y,f}$ and $F_{y,r}$ in (1)-(3) with (6) and using $\begin{bmatrix} v_x & v_y & \dot{\psi} & \Delta\psi & \Delta y \end{bmatrix}^T$ as state vector, the lateral distance Δy as controlled output y, the steering angle δ as control input u and the path's curvature κ (provided by a path planner) as system disturbance z, the resulting nonlinear prediction model can be written in state space representation

$$\dot{\boldsymbol{x}}(t) = \boldsymbol{f}(\boldsymbol{x}(t), u(t), z(t)) \tag{9}$$

$$y(t) = g(\boldsymbol{x}(t)) \tag{10}$$

where $\boldsymbol{x} = \begin{bmatrix} v_x & v_y & \dot{\psi} & \Delta\psi & \Delta y \end{bmatrix}^T$, $u = \delta$ and $z = \kappa$. To be used in the predictive control algorithm, the nonlinear prediction model (9)-(10) has to be linearized at a particular operating point $(\boldsymbol{x}_0, u_0, z_0)$ and to be transformed into a discrete-time representation. Finally, the resulting discrete-time linear affine prediction model can be written as

$$\boldsymbol{x}_{k+1} = \boldsymbol{A}_k\boldsymbol{x}_k + \boldsymbol{B}_k u_k + \boldsymbol{E}_k z_k + \boldsymbol{\Gamma}_k \tag{11}$$

$$y_k = \begin{bmatrix} 0 & 0 & 0 & 0 & 1 \end{bmatrix}\boldsymbol{x}_k = \Delta y_k \tag{12}$$

where $\boldsymbol{A}_k \in \mathbb{R}^{5\times5}$, $\boldsymbol{B}_k \in \mathbb{R}^5$, $\boldsymbol{E}_k \in \mathbb{R}^5$ and $\boldsymbol{\Gamma}_k \in \mathbb{R}^5$ are time-variant matrices resp. vectors with respect to time k. In this context, $\boldsymbol{A}_k$ denotes the system matrix, $\boldsymbol{B}_k$ the input matrix, $\boldsymbol{E}_k$ describes the influence of the system disturbance z on the state variables and $\boldsymbol{\Gamma}_k$ denotes an affine term that results from the linearization of (9)-(10).

III. PREDICTIVE CONTROL

In this section, the predictive control approach for lateral vehicle guidance is introduced consecutively. First, the predictive control problem to follow an evasion path with minimum deviations is formulated as constrainted quadratic optimization problem. Second, the authors propose an algorithm to assign the upper and lower sideslip angle bounds to allow vehicle stabilization at the limits of vehicle dynamics. Third, the reference control scheme, subsequently referred to as LTV-MPC$_{ref}$, that employs linearizations of the nonlinear prediction model (9)-(10) which remain unchanged over the prediciton horizon is presented. Finally, the estimation based LTV-MPC controller, subsequently referred to as LTV-MPC$_{est}$, that employs successive linearizations of the nonlinear prediction model over the prediction horizon is described in detail. For both controllers, it is assumed that the state variables are fully measurable so that no state observer is required. In the following, H_u denotes the length of the control horizon, H_p the length of the prediction horizon and $\{\cdot\}_{(k+j|k)}$ the prediction at time k of variable $\{\cdot\}$ at time $k+j$.

A. Predictive control problem

As mentioned in section II-A, the main objective of the controller is to minimize the lateral distance Δy by applying the steering angle δ to follow the evasion path in an optimal way. Consequently, the reference value of the controlled output $y = \Delta y$ is set to zero. The system disturbance κ is provided by a path planner for the entire prediction horizon. In this context, κ_k is determined according to Fig. 1 while $\kappa_{(k+j|k)}, j = 1, ..., H_p - 1$ is estimated assuming that the vehicle follows the evasion path without any deviations. In order to determine the control input $u_{(k|k)} = u_{k-1} + \Delta u_{(k|k)}$, i.e. the steering angle δ, that is applied to the plant at the next time instant, a constrainted quadratic optimization problem has to be solved. Using the cost function

$$J = Q \cdot \sum_{j=1}^{H_p} {y_{(k+j|k)}}^2 + R \cdot \sum_{j=0}^{H_u-1} {\Delta u_{(k+j|k)}}^2 + \rho_f \cdot \epsilon_f + \rho_r \cdot \epsilon_r \qquad (13)$$

the constrainted quadratic optimization problem can be formulated as:

$$\min_{\boldsymbol{\Delta u}, \epsilon_f, \epsilon_r} J \qquad (14a)$$

subject to

$$\Delta\delta_{min} \leq \Delta u_{(k+j|k)} \leq \Delta\delta_{max}, \qquad j = 0, ..., H_u - 1 \qquad (14b)$$

$$\delta_{min} \leq u_{(k+j|k)} \leq \delta_{max}, \qquad j = 0, ..., H_u - 1 \qquad (14c)$$

$$\alpha_{f,min,(k+j|k)} - \epsilon_f \leq \alpha_{f,(k+j|k)}, \qquad j = 0, ..., H_p \qquad (14d)$$

$$\alpha_{f,max(k+j|k)} + \epsilon_f \geq \alpha_{f,(k+j|k)}, \qquad j = 0, ..., H_p \qquad (14e)$$

$$\alpha_{r,min,(k+j|k)} - \epsilon_r \leq \alpha_{r,(k+j|k)}, \qquad j = 1, ..., H_p \qquad (14f)$$

$$\alpha_{r,max,(k+j|k)} + \epsilon_r \geq \alpha_{r,(k+j|k)}, \qquad j = 1, ..., H_p \qquad (14g)$$

$$\epsilon_f \geq 0, \ \epsilon_r \geq 0 \qquad (14h)$$

where $\boldsymbol{\Delta u} = [\Delta u_{(k|k)}, ..., \Delta u_{(k+H_u-1|k)}]^T$. Constraints (14b)-(14c) are introduced to take actuator limitations into account. In particular, (14c) is employed to limit the abolute steering angle while (14b) limits the maximum and minimum steering angle shift per time step. Soft constraints (14d)-(14h) on the tire sideslip angles are used to keep the vehicle in stable driving conditions. As the tire sideslip angles at the front tire are influenced instantaneously by the steering angle, see (7), constraints (14d)-(14e) on α_f have additionally to be defined for $j = 0$. A detailed description of the assignment of the maximum and minimum values of the tire sideslip angles, i.e. $\alpha_{f,max/min}$ resp. $\alpha_{r,max/min}$ in (14d)-(14g), will be given in section III-B. In order to ensure feasibility of the optimization problem, the slack variables ϵ_f and ϵ_r are introduced. Finally, Q, R, ρ_f and ρ_r in (13) denote weighting coefficients.

B. Assignment of tire sideslip angle bounds

In [6], constraints (14d)-(14h) have already been introduced to limit the tire sideslip angles to the linear region of the tire model. Subsequently, an extension of [6] will be presented which aims at guiding the vehicle at the limits of vehicle dynamics. As LTV-MPC$_{est}$ employs successive linearizations of (9)-(10) over the prediction horizon, the authors propose to define $\alpha_{f,max/min}$ and $\alpha_{r,max/min}$ in such a way that they depend on the operating point $(\boldsymbol{x}_0,\ u_0,\ z_0)$ at time $k+j$ with respect to the prediction horizon. In contrast, for LTV-MPC$_{ref}$ the operating point and thus the values for $\alpha_{f,max/min}$ and $\alpha_{r,max/min}$ remain unchanged over the prediction horizon. Therefore, these bounds are determined once at time k such that $\alpha_{i,max/min,(k+j|k)} = const., \forall j,\ i \in \{f, r\}$. Before the upper and lower bounds are defined, the linearization of the Pacejka tire model (6) is investigated at the operating point $(\alpha_{i,0}, F_{y,i,0})$

$$F_{y,i} = (\alpha_i - \alpha_{i,0}) \cdot k_{\alpha_i} + F_{y,i,0},\ i \in \{f, r\} \qquad (15)$$

where k_{α_i} denotes the linearization coefficient and $\alpha_{i,0}$ resp. $F_{y,i,0}$ denote the values for α_i resp. $F_{y,i}$ at the operating point $(\boldsymbol{x}_0,\ u_0,\ z_0)$. As depicted in Fig. 2, using (15) (i.e. the red dashed line) would cause lateral tire forces that are larger resp. less than the maximum resp. minimum feasible force $F_{y,i}(\alpha_{i,PMF,max/min})$ for $\alpha_i > \alpha_{i,LIN,max}$

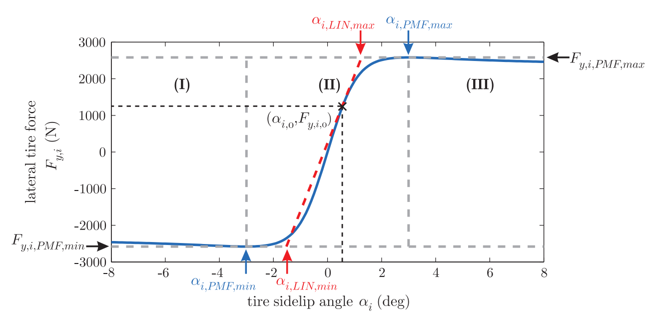

Fig. 2. Assignment of tire sideslip angle constraints (solid blue line: Pacejka tire model, dashed red line: linearization at a particular operating point)

resp. $\alpha_i < \alpha_{i,LIN,min}$. In this context, $\alpha_{i,PMF,max/min}$ denotes the tire sideslip angle that causes the maximum resp. minimum lateral tire force with respect to the Pacejka tire model. In order to prevent the predictive controller from assuming lateral forces that are not physically feasible and to ensure that tires saturate in a conservative way, maximum and minimum values of the tire sideslip angles are defined considering the operating point ($\boldsymbol{x}_0$, u_0, z_0) at time $k+j$ of the predicition horizon. In particular, if $\alpha_{i,0,(k+j|k)}$ is located in the stable region of the tire model (i.e. $\alpha_{i,PMF,min} < \alpha_{i,0,(k+j|k)} < \alpha_{i,PMF,max}$, see region II in Fig. 2), the tire sideslip angle bounds are chosen as

$$\alpha_{i,max,(k+j|k)} = \min\{\xi \cdot \alpha_{i,PMF,max}, \quad \alpha_{i,LIN,max,(k+j|k)}\} \tag{16}$$

$$\alpha_{i,min,(k+j|k)} = \max\{\xi \cdot \alpha_{i,PMF,min}, \quad \alpha_{i,LIN,min,(k+j|k)}\} \tag{17}$$

where

$$\alpha_{i,LIN,max/min,(k+j|k)} = \alpha_{i,0,(k+j|k)} + (F_{y,i,PMF,max/min} - F_{y,i,0,(k+j|k)})/k_{\alpha_i,(k+j|k)} \tag{18}$$

denotes the tire sideslip angle that corresponds to the intersection of the tangent to $F_{y,i}$ at the operating point $(\alpha_{i,0}, F_{y,i,0})$, i.e. the red dashed line in Fig. 2, and $F_{y,i,PMF,max/min}$. As extensive analysis has shown that it is reasonable if tire sideslip angles are slightly less than $\alpha_{i,PMF,max}$ resp. larger than $\alpha_{i,PMF,min}$, $0 < \xi < 1$ is additionally introduced in (16)-(17). Especially, if (2) resp. (3) are linearized close to $\alpha_{f,PMF,max/min}$, the linearization coefficient of the steering angle δ changes its sign and may thus cause false control actions. Obviously, ξ has to be chosen close to one to operate at the limits of vehicle dynamics. If tires are saturated (i.e. $\alpha_{i,0,(k+j|k)} \leq \alpha_{i,PMF,min}$ resp. $\alpha_{i,0,(k+j|k)} \geq \alpha_{i,PMF,max}$, see region I resp. III in Fig. 2), the main objective is to lead the tire sideslip angles back into the stable region of the tire model. Therefore, the upper and lower bounds are chosen as

$$\alpha_{i,max/min,(k+j|k)} = \xi \cdot \alpha_{i,PMF,max/min}. \tag{19}$$

C. Reference LTV-MPC controller

The reference control scheme LTV-MPC$_{ref}$ determines a linearization of the nonlinear prediction model (9)-(10) at the operating point

$$(\boldsymbol{x}_0 = \boldsymbol{x}_k,\ u_0 = \delta_{k-1},\ z_0 = \kappa_k) \tag{20}$$

once the controller is executed at time k. In this context, $\boldsymbol{x}_k$ denotes the feedback of the state variables at time k, δ_{k-1} the control input that has been applied to the plant at time $k-1$ and κ_k the system disturbance at time k. The resulting discrete-time linear affine prediction model (11)-(12), which remains unchanged over the prediction horizon, is used to determine the free response of the plant and to formulate the constrainted quadratic optimization problem (14).

D. Estimation-based LTV-MPC controller

1) Basic principles: Due to the fact that dynamic time constants of the plant are quite small compared to the length of the prediction horizon, linearizations of (9)-(10) become less accurate after a short time period if the vehicle operates near the limits of vehicle dynamics. In order to overcome this problem, the main idea of LTV-MPC$_{est}$ is to successively estimate the control input δ_{est} that is assumed to be applied by the predictive controller to follow the evasion path as well as the resulting state variables $\boldsymbol{x}_{est}$ to successively determine linearizations of (9)-(10) over the prediction horizon. Therefore, it is assumed that the evasion path is physically feasible and can be followed by the controller. In particular, the estimated control input $\delta_{est,(k+j-1|k)}$ and the path's curvature $\kappa_{(k+j-1|k)}$ are used to integrate (1)-(3) numerically in order to obtain the estimated state variables $\boldsymbol{x}_{est,(k+j|k)}$ for $j = 1, ..., H_p - 1$. As it is assumed that the evasion path can be followed by the controller, the estimated values of the remaining state variables $\Delta\psi_{est,(k+j|k)}$ and $\Delta y_{est,(k+j|k)}$ are expected to be very small and therefore assigned to zero. It has to be stated that the estimation algorithm provides the best results if the evasion path is physically feasible and the control horizon H_u is of the same length as the prediction horizon H_p. For $H_u < H_p$, the solution of the constrainted quadratic optimization problem (14) will be determined in such a way that deviations from the evasion path are minimized over the prediction horizon while the control input can only be changed over a shorter control horizon. In contrast, the estimation algorithm changes the control input over the entire prediction horizon. Nevertheless, simulation results show that a rather satisfying control perfomance can be obtained for $H_u < H_p$.

2) Successive linearization: Based on the estimation of the control input δ_{est} and the state variables $\boldsymbol{x}_{est}$, the operating points, used for linearization of (9)-(10), are

$$(\boldsymbol{x}_0 = \boldsymbol{x}_k,\ u_0 = \delta_{k-1},\ z_0 = \kappa_k) \tag{21}$$

at time k and

$$(\boldsymbol{x}_0 = \boldsymbol{x}_{est,(k+j|k)},\ u_0 = \delta_{est,(k+j-1|k)},\ z_0 = \kappa_{(k+j|k)}) \tag{22}$$

at time $k+j$, $j = 1, ..., H_p - 1$ with respect to the prediction horizon. In this context, $\boldsymbol{x}_k$ denotes the feedback of the state variables at time k, δ_{k-1} the control input that has been applied to the plant at time $k-1$ and κ_k the system disturbance at time k. Consequently, the matrices resp. vectors $\boldsymbol{A}_{(k+j|k)}$, $\boldsymbol{B}_{(k+j|k)}$, $\boldsymbol{E}_{(k+j|k)}$ and $\boldsymbol{\Gamma}_{(k+j|k)}$ in (11)-(12) are obtained for $j = 0, ..., H_p - 1$. These are subsequently used to formulate the constrainted quadratic optimization problem (14). In contrast to LTV-MPC$_{ref}$, the free response of the plant is determined by integrating (1)-(5) numerically. In order to reduce numerical errors, a higher order integration technique is employed.

3) Control input estimation: In the following, the algorithm to estimate the control input δ_{est} that is assumed to be applied by the predictive controller to follow the evasion path is described in detail. As a first step, the algorithm determines the difference angle between the vehicle and the evasion path at the next time step of the prediction horizon. Subsequently, the required steering angle that causes a yaw rate, necessary to compensate the difference angle within a single time step, is computed. More precisely, at each time step $k+j$, $j=0,...,H_p-2$ of the prediction horizon the difference angle $\Delta\psi_{(k+j+1|k)}$ at the next time step is determined successively by applying the discrete-time linear affine prediction model (11)

$$\begin{aligned}\Delta\psi_{(k+j+1|k)} &= a_{4,1}\cdot v_{x,(k+j|k)} + a_{4,2}\cdot v_{y,(k+j|k)} \\ &+ a_{4,3}\cdot\dot{\psi}_{(k+j|k)} + a_{4,4}\cdot\Delta\psi_{(k+j|k)} \\ &+ e_4\cdot\kappa_{(k+j|k)} + \gamma_4\end{aligned} \tag{23}$$

where $a_{m,n}$, e_m and γ_m denote the entries of $\boldsymbol{A}_{(k+j|k)}$, $\boldsymbol{E}_{(k+j|k)}$ and $\boldsymbol{\Gamma}_{(k+j|k)}$ in (11) at row m resp. column n. Furthermore, the state variables for $j=0$ are known from the feedback of the state variables at time k. In order to compensate the difference angle within a single time step, the desired yaw rate has to be chosen as

$$\dot{\psi}_{ref,(k+j+1|k)} = \Delta\psi_{(k+j+1|k)}/T_s \tag{24}$$

where T_s denotes the sampling interval. The required steering angle, that has to be applied at the current time step, can be determined by reorganizing the disrecte-time linear affine equation for $\dot{\psi}_{(k+j+1|k)}$ in (11) with respect to $\delta_{(k+j|k)}$

$$\begin{aligned}\delta_{est,(k+j|k)} = (&\dot{\psi}_{ref,(k+j+1|k)} \\ &- a_{3,1}\cdot v_{x,(k+j|k)} - a_{3,2}\cdot v_{y,(k+j|k)} \\ &- a_{3,3}\cdot\dot{\psi}_{(k+j|k)} - \gamma_3)/b_3\end{aligned} \tag{25}$$

where $a_{m,n}$, b_m and γ_m denote the entries of $\boldsymbol{A}_{(k+j|k)}$, $\boldsymbol{B}_{(k+j|k)}$ and $\boldsymbol{\Gamma}_{(k+j|k)}$ in (11) at row m resp. column n. In this paper, the case of $b_3=0$ is neglegted as this will only occur if the vehicle cannot be stabilized any more. If b_3 is close to zero, δ_{est} will become quite large and has thus to be adjusted as described subsequently. Furthermore, the steering angle $\delta_{est,(k+j|k)}$ that is assumed to be chosen by the predictive controller has to be verified against optimization constraints (14b)-(14g) in order to obtain an appropiate estimation result. As it is not possible to fulfill all the constraints, the following steps are conducted successively.

1) $\delta_{est,(k+j|k)}$ is limited to $\delta_{max/min}$ in (14c).
2) $\delta_{est,(k+j|k)}$ is adjusted with respect to $\Delta\delta_{max/min}$ in (14b) such that $\Delta\delta_{est,(k+j|k)} \leq \eta\cdot\Delta\delta_{max}$ resp. $\Delta\delta_{est,(k+j|k)} \geq \eta\cdot\Delta\delta_{min}$. In contrast to optimization problem (14), $\Delta\delta_{est,(k+j|k)}$ does not result from a global optimization and thus η has to be chosen larger than 1 as $\eta=1$ has turned out to be too conservative.
3) According to (19), $\delta_{est,(k+j|k)}$ is corrected such that $\alpha_{f,(k+j+1|k)}$ is located in the stable region of the tire model. In this context, $\alpha_{f,(k+j+1|k)}$ is predicted using $\delta_{est,(k+j|k)}$ and $\boldsymbol{x}_{est,(k+j|k)}$ as well as the linearization of (1)-(5) and (7) at time $k+j$. If $\alpha_{f,(k+j+1|k)}$ is larger than $\xi\cdot\alpha_{i,PMF,max}$ resp. less than $\xi\cdot\alpha_{i,PMF,min}$, $\delta_{est,(k+j|k)}$ is adjusted such that $\alpha_{f,(k+j+1|k)}$ is equal to $\xi\cdot\alpha_{i,PMF,max/min}$. Thus, this correction step aims at determining an operating point for the linearization of (1)-(5) at time $k+j+1$ such that the tire sideslip angle at the front axle is located in the stable region of the tire model.

Furthermore, additional effort has been made to predict $\alpha_{r,(k+j+1|k)}$ and finally correct $\delta_{est,(k+j|k)}$ such that both sideslip angles remain in the stable region. But as a further improvement could not be achieved, this final correction step is omitted as the vehicle can be kept in stable driving conditions by appropiately choosing weighting coefficents ρ_f and ρ_r. Subsequently, $\delta_{est,(k+j|k)}$ can be used, as described above, to estimate the state variables $\boldsymbol{x}_{est,(k+j+1|k)}$.

IV. SIMULATION RESULTS

In order to compare the performance of LTV-MPC$_{est}$ and LTV-MPC$_{ref}$, a co-simulation of IPG CarMaker and MATLAB/Simulink™ is employed. In particular, the MPC controllers are implemented in MATLAB/Simulink™ while IPG CarMaker provides complex multi-body vehicle models and several validated tire datasets that are used as validation model. The required parameters of the prediction model are either provided by IPG CarMaker or have been identified in simulation runs (i.e. tire parameters). The test scenarios are explicitly chosen to evaluate the control performance of LTV-MPC$_{est}$ at the limits of vehicle dynamics. Similar to [6], a double lane change maneuver on a snow covered road ($\mu=0.3$) is investigated for an initial velocity of $v_{COG,0}=14\,\mathrm{m/s}$ resp. $v_{COG,0}=18\,\mathrm{m/s}$. For $v_{COG,0}=14\,\mathrm{m/s}$, the evasion path is physically feasible for almost the entire maneuver. Only for a short time interval, the maximum feasible lateral acceleration is temporarily exceeded by $1\,\mathrm{m/s^2}$. In contrast, for $v_{COG,0}=18\,\mathrm{m/s}$ the evasion path becomes physically unfeasible for almost

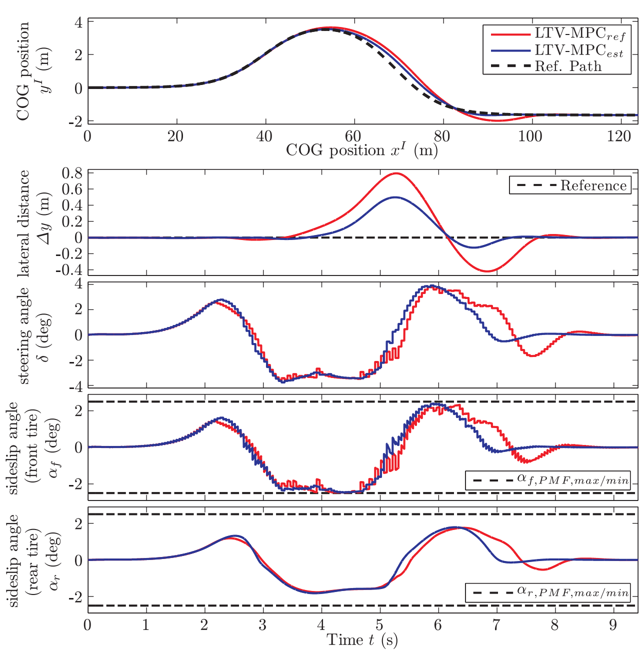

Fig. 3. Simulation results for $v_{COG,0}=14\,\mathrm{m/s}$

the entire maneuver. In this way, it is investigated if both controllers are able to stabilize the vehicle even if the path planner provides an unfeasible path. In fact, this will not be the case if the path planner works correct. To assess the practical applicability of LTV-MPC$_{est}$, H_u ist chosen shorter than H_p. For each simulation that has been conducted, the following parameters have been used: $T_s = 0.05\,\mathrm{s}$, $H_u = 15$, $H_p = 25$, $Q = 1$, $R = 100$, $\rho_f = 1000$, $\rho_r = 1000$, $\xi = 0.99$, $\delta_{max/min} = \pm 10°$, $\Delta\delta_{max/min} = \pm 0.9°$, $\eta = 2.8$.

Fig. 3 shows the simulation results for an initial velocity of $v_{COG,0} = 14\,\mathrm{m/s}$. In order to evaluate and compare LTV-MPC$_{est}$ and LTV-MPC$_{ref}$, the rms error Δy_{rms} as well as the maximum deviation Δy_{max} from the evasion path are investigated to assess the overall resp. the local control performance. Comparing both controllers, an improved control performance of LTV-MPC$_{est}$ compared to LTV-MPC$_{ref}$ can be observed. In particular, the rms error of LTV-MPC$_{est}$ is 44.4% less compared to LTV-MPC$_{ref}$, see Table II. The maximum deviation Δy_{max}, which occurs at $t = 5.3\,\mathrm{s}$, can be reduced by 36.7% resp. 0.29 m. Even the deviation at the end of the maneuver is significantly less and thus the entire maneuver is ended 0.7 s earlier. Finally, both controllers are able to stabilize the vehicle at the limits of vehicle dynamics.

Simulation results for an initial velocity of $v_{COG,0} = 18\,\mathrm{m/s}$ are depicted in Fig. 4. Although estimation results of LTV-MPC$_{est}$ degrade as the evasion path is physically unfeasible, the rms error of LTV-MPC$_{est}$ is still 19.2% less compared to LTV-MPC$_{ref}$. The maximum deviation Δy_{max}, which can be observed at $t = 4.3\,\mathrm{s}$, is 16.3% resp. 0.48 m less. Furthermore, both controllers have the ability to prevent the vehicle from getting instable, even when the tire sideslip angles leave the stable region of the tire model temporarily.

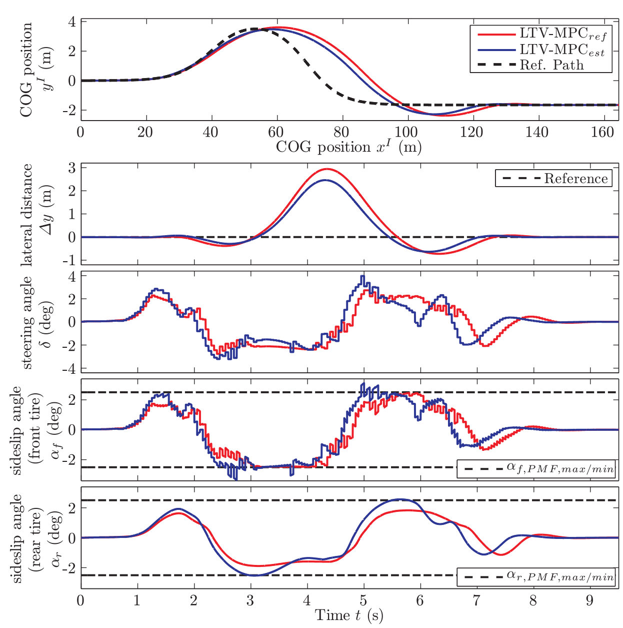

Fig. 4. Simulation results for $v_{COG,0} = 18\,\mathrm{m/s}$

TABLE II

CONTROLLER PERFORMANCE

	$v_{COG,0}$(m/s)	Δy_{rms} (m)	Δy_{max} (m)
LTV-MPC$_{ref}$	14	0.27	0.79
LTV-MPC$_{est}$	14	0.15	0.50
Improvement (%)		44.4	36.7
LTV-MPC$_{ref}$	18	0.99	2.94
LTV-MPC$_{est}$	18	0.80	2.46
Improvement (%)		19.2	16.3

V. CONCLUSIONS AND FUTURE WORKS

In this paper, a LTV-MPC approach for lateral vehicle guidance by front steering has been presented. Due to the fact that linearizations of the nonlinear prediction model become less accurate after a short time period if the vehicle operates near the limits of vehicle dynamics, a LTV-MPC controller has been proposed that uses successive linearizations over the prediciton horizon. In order to assess the control performance of the proposed controller, it is compared to a LTV-MPC controller that uses linearizations that remain unchanged over the prediction horizon. Simulation results show that an improved control performance can be achieved by the estimation based approach.

As far as future work is concerned, the authors are going to implement an appropiate state observer that can be employed at the limits of vehicle dynamics. Furthermore, additional effort will be made to improve the quality of the estimation algorithm, especially when deviations from the evasion path increase.

REFERENCES

[1] R. Isermann and R. Mannale and K. Schmitt, "Collision avoidance systems PRORETA: situation analysis and intervention control", *in IFAC Symposium Advances in Automotive Control*, Munich, Germany, 2010.

[2] A. Katriniok and M. Reiter and F. Christen and L. Eckstein, "Collision Avoidance using Galileo - The automotiveGATE as Development and Testing Center for Galileo based Applications", *in Aachener Kolloquium Fahrzeug- und Motorentechnik*, Aachen, Germany, 2010, pp. 1689-1700.

[3] J. Maciejowski, *Predictive Control with Constraints*, Prentice Hall, Harlow, 2002.

[4] S. Di Cairano and H. Tseng and D. Bernardini and A. Bemporad, "Steering Vehicle Control by Switched Model Predictive Control", *in IFAC Symposium Advances in Automotive Control*, 2010.

[5] T. Besselmann and M. Morari, "Hybrid Parameter-varying Model Predictive Control for Autonomous Vehicle Steering", *in European Journal of Control*, Vol. 14/5, 2008, pp. 418-431.

[6] P. Falcone and F. Borrelli and J. Asgari and H. Tseng and D. Hrovat, "Predictive Active Steering Control for Autonomous Vehicle Systems", *in IEEE Transactions on Control Systems Technology*, Vol. 15/3, 2007, pp. 566-580.

[7] M. Mitschke and H. Wallentowitz, *Dynamik der Kraftfahrzeuge*, Springer Verlag, Berlin, 2004.

[8] G.C. Keßler and J.P. Maschuw and N. Zambou and A. Bollig, "Concept for the Generation of Reference Variables and Model-Based Predictive Control for the Lateral Guidance of Heavy-Duty Vehicle Platoons", *in Automatisierungstechnik*, Vol. 55/6, 2007, pp. 298-305.

[9] H. Pacejka and E. Bakker, "The magic formular tire model", *in Vehicle System Dynamics: International Journal of Vehicle Mechanics and Mobility*, Vol. 21/1, 1992, pp. 1-18.